4814 *Macromolecules* **2010**, *43*, 4814–4821
DOI: 10.1021/ma100508c

Macromolecules
ARTICLE

# Restoring Thermorheological Simplicity in Miscible Polymer Blends: How Many Hydrogen Bonds Are Required?

**Ashish N. Gaikwad,[‡] Andrea Choperena,[§] Paul C. Painter,[§] and Timothy P. Lodge*[,†,‡]**

[†]*Department of Chemistry, and* [‡]*Department of Chemical Engineering & Materials Science, University of Minnesota, Minneapolis, Minnesota 55455, and* [§]*Department of Materials Science and Engineering, Pennsylvania State University, University Park, Pennsylvania 16802*

*Received March 5, 2010; Revised Manuscript Received April 22, 2010*

ABSTRACT: The linear viscoelastic properties of blends of poly(vinyl methyl ether) (PVME) with poly(styrene) (PS), poly(styrene-*stat*-vinylphenol) (PSVPh) copolymers, and poly(vinylphenol) (PVPh) in different proportions were measured over a wide temperature range (0−160 °C). All blends were miscible over the temperature and composition ranges covered. The amount of hydrogen bonding was tuned by using copolymers with varying mole fractions of vinylphenol units (10%, 20%, and 50%). The time−temperature superposition principle (tTS) was used to create master curves from the rheological data. For some PS/PVME and PSVPh/PVME blends there was a clear failure of tTS. In contrast, tTS was successful for all the PVPh/PVME blends and PSVPh/PVME blends with higher vinylphenol content, despite much higher differences between the component $T_g$s. These results confirm that the dynamic response of two polymers can be effectively coupled in the presence of sufficient hydrogen-bonding interactions, whereby the temperature dependences of the two-component relaxation times become equivalent. By using an established model for predicting the extent of hydrogen bonding, the concentration of hydrogen bonds necessary to couple the dynamic behavior, as reflected by the success of tTS, was estimated. The size of the associated "control volume" is comparable to the Kuhn length.

## Introduction

Miscible polymer blends have been a topic of great interest due to both their potential commercial usefulness and as a test of current understanding of polymer thermodynamics and dynamics. Even after many theoretical and experimental studies,[1−50] the dynamic behavior of polymer blends is still incompletely understood compared to the corresponding pure homopolymers. Typically, the temperature and composition dependences of the monomeric friction factor $\zeta$, characterizing the friction experienced by a polymer segment, are distinct for each component in the blend. This, in turn, leads to differing temperature and composition dependences for the dynamics for each component, at both the segmental and the global chain level. Therefore, although the polymers are thermodynamically miscible, this dynamic heterogeneity can lead to the failure of time−temperature superposition (tTS), indicating that the blend components are relaxing at a different rates.[3−9] The broadening of the glass transition,[10−13] including the observation of two distinct transitions, and complex dependences of blend viscosity on composition[14−27] are other interesting and related characteristics of miscible blends.

Many of the dynamics studies have been carried out on blends where the components do not form hydrogen bonds, such as poly(ethylene oxide) (PEO)/poly(methyl methacrylate) (PMMA),[3,7] poly(styrene) (PS)/poly(vinyl methyl ether) (PVME),[31−37] and poly(isoprene)/poly(vinylethylene).[10,38−40] Thermorheological complexity has been observed for these nearly athermal blends when there is substantial dynamic asymmetry, i.e., a large difference between the glass transition temperatures of the pure blend components, $\Delta T_g$. On the other hand, there are many miscible pairs in which the two components can interact via hydrogen bonding, including poly(vinylidene fluoride)/PMMA,[41,42] poly(styrene-*co*-vinylphenol) (PSVPh)/poly(propylene carbonate),[43] PSVPh/poly(vinylpyridine),[44,57] PVPh/PEO,[45−47] PVPh/PVME,[48−50] and PVPh/PMMA.[51] It is possible that the presence of strong hydrogen bonding could lead to the coupling of the dynamic responses of the component chains, such that "dynamic homogeneity" and the successful application of tTS would be restored.

Thus, it is interesting to explore a series of blends where the number of hydrogen-bonding interactions can be systematically tuned. The model system of PVME as one component, and PS or PVPh as the other, provides such an opportunity. If a statistical copolymer of styrene and 4-vinylphenol is blended with pure PVME, then the level of hydrogen-bonding interactions can be controlled by simply changing the vinylphenol content in the copolymer as well as by changing the blend composition. As strong hydrogen-bonding interactions are present between the hydroxyl groups of PVPh and the ether oxygens of PVME,[52] styrene simply acts as a hydrogen bond diluent in this system, while miscibility is expected across the entire composition range. Thermorheological complexity has been well-documented for PS/PVME blends,[33,37,53−57] whereas it has been reported[49,50] that hydrogen-bonding interactions in PVPh/PVME blends can lead to coupled segmental and/or chain relaxation. In this report we document how increasing the number of hydrogen bonds restores tTS. By applying a well-established model for hydrogen bonding in polymer blends, we are able to relate the success of tTS to a critical concentration of hydrogen bonds.

## Experimental Section

**Materials.** Poly(vinylphenol) (PVPh) with $M_w \approx 10\,000$ g/mol and a polydispersity index (PDI) of 1.1 was purchased from Sigma-Aldrich, and poly(styrene) (PS) with $M_w \approx 12\,000$ g/mol

*Author for correspondence. E-mail: lodge@umn.edu.

 Published on Web 05/03/2010 

and a PDI of 1.05 was synthesized by Davidock.[59] Three statistical copolymers of styrene and vinylphenol were synthesized by nitroxide-mediated polymerization (NMP) using 4-methoxy-2,2,6,6-tetramethylpiperidine-1-oxyl (MTEMPO) as an initiator and benzoyl peroxide as a co-initiator, both purchased from Sigma-Aldrich. Styrene and *p*-*tert*-butoxystyrene were used as starting materials. After polymerization the *tert*-butoxy groups were removed by hydrolysis with concentrated hydrochloric acid to leave the phenolic hydroxyl group. As confirmed via $^1$H NMR spectroscopy, greater than 99% of the *tert*-butoxy groups were removed during deprotection. More details of the synthesis procedure are provided in the Supporting Information.[60,61] All the copolymers had $M_w \approx 10\,000$ g/mol and PDI $\approx 1.1$. They are referred to as PSVPh90, PSVPh80, and PSVPh50, where the number denotes the mole percent of styrene in the copolymer.

Poly(vinyl methyl ether) (PVME) with $M_w \approx 90\,000$ g/mol was purchased from Scientific Polymer Products. In order to reduce the polydispersity, fractionation was carried out with a toluene (solvent)/*n*-hexane (nonsolvent) mixture. *n*-Hexane was added dropwise to a 2 wt % solution of PVME in toluene, until the solution became sufficiently cloudy. The solution was subsequently heated until it once again became clear ($T \approx 313$ K). It was then allowed to cool slowly to room temperature and separate into two layers. The bottom layer was recovered and dried under nitrogen.

**Table 1. Properties of Polymers**

| polymer | VPh units[a] (mol %) | $M_w$[b] (kg/mol) | polydispersity[b] | $T_g$[c] (°C) |
|---|---|---|---|---|
| PVME | | 70 | 1.3 | −25 |
| PS | | 12 | 1.05 | 100 |
| PVPh | 100 | 10 | 1.1 | 174 |
| PSVPh50 | 50 | 10 | 1.12 | 143 |
| PSVPh80 | 20 | 9.5 | 1.08 | 114 |
| PSVPh90 | 10 | 9.5 | 1.1 | 101 |

[a] By $^1$H NMR analysis. [b] By SEC measurements. [c] From DSC measurements.

Size exclusion chromatography (SEC) was used to determine molecular weights and polydispersities. The separation was achieved by passing the solution through three Phenomenex Phenogel columns with the pore sizes of $10^3$, $10^4$, and $10^5$ Å, using THF as a mobile phase. A refractive index (RI) detector (Wyatt Technology OPTILAB) and a light scattering (LS) detector (Wyatt Technology DAWN) were used to determine absolute molecular weights of the polymers. $^1$H NMR measurements were carried out on Varian solution state spectrometer (300 MHz). The ratio of styrene and *p*-*tert*-butoxystyrene in the copolymer was calculated based on peak areas. Detailed calculations, along with representative spectra before and after deprotection, are given in the Supporting Information. The glass transition temperatures, molecular weights, and polydispersity indexes ($M_w/M_n$) of the polymers used in this study are listed in Table 1.

**Blend Preparation.** Blends were prepared by codissolving appropriate amounts of polymers in THF with 0.5 wt % of the antioxidant 2,6-di-*tert*-butyl-4-methylphenol. Solutions were then stirred overnight, and solvent was removed by evaporation under flowing nitrogen. All the blends were further dried in a vacuum oven above the $T_g$ of the blend, until constant weight was achieved. All blend compositions in this article are reported as weight percent.

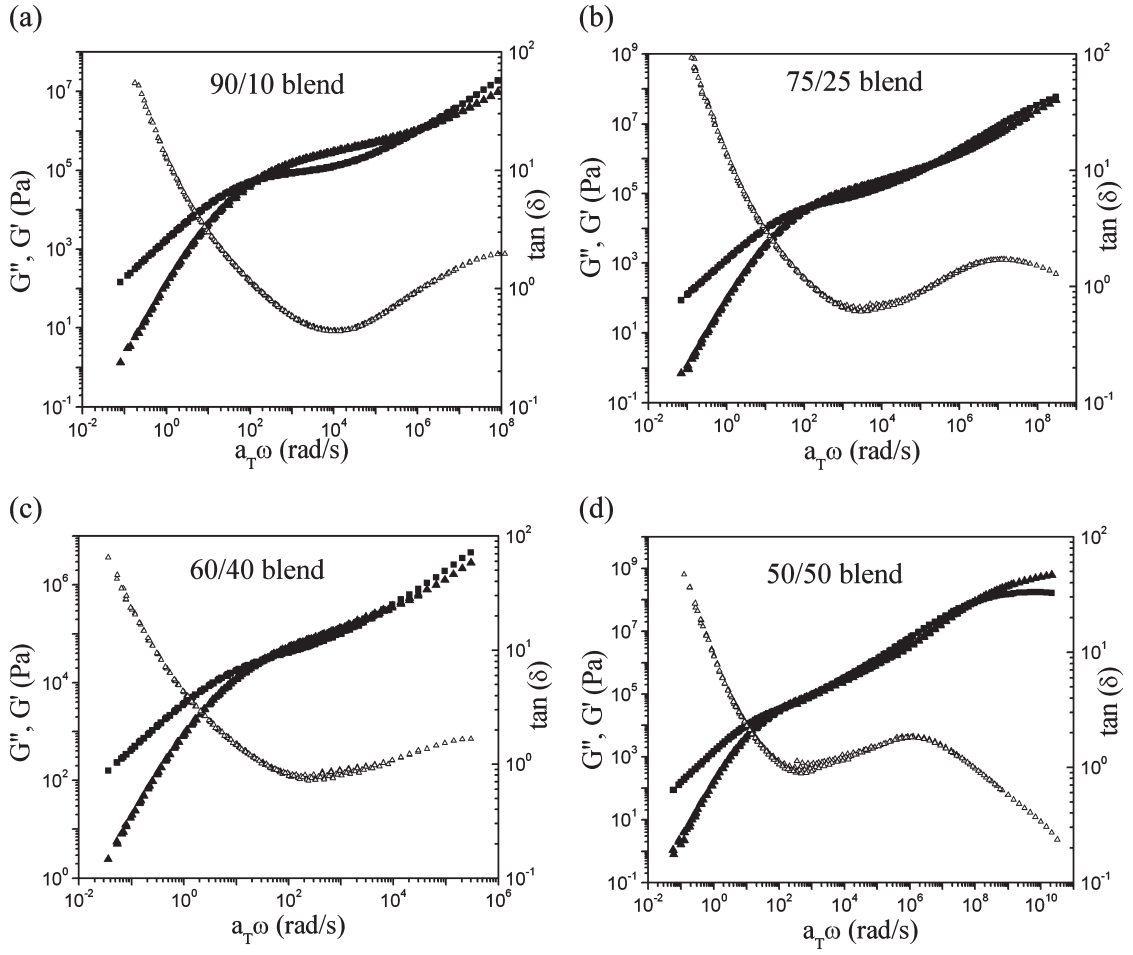


**Figure 1.** Master curves of $G'$ (▲), $G''$ (■), and tan($\delta$) (Δ) for PVME/PSVPh90 blends: (a) 90% PVME; (b) 75% PVME; (c) 60% PVME; (d) 50% PVME. The reference temperature is 100 °C for each curve.

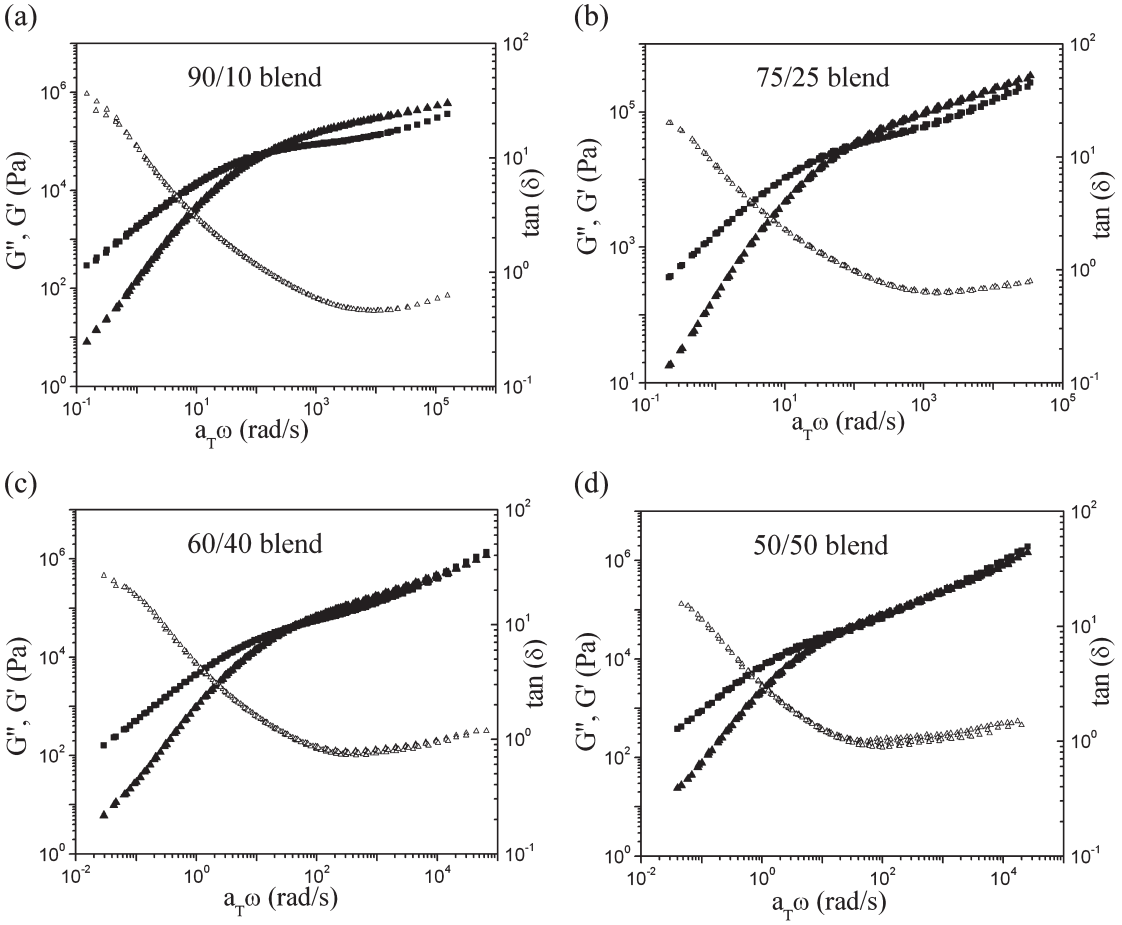


**Figure 2.** Master curves of $G'$ (▲), $G''$ (■), and tan($\delta$) ($\Delta$) for PVME/PSVPh80 blends: (a) 90% PVME; (b) 75% PVME; (c) 60% PVME; (d) 50% PVME. The reference temperature is 100 °C for each curve.

**Differential Scanning Calorimetry.** DSC samples were prepared by sealing ~10 mg of material in aluminum hermetic pans, provided by TA Instruments. DSC experiments were carried out with a TA Instruments Q1000 equipped with a liquid nitrogen cooling system. An empty hermetic pan was used as the reference in every case. The instrument was calibrated using an indium standard (melting point −156.6 °C), and errors were found to be less than 2% in the heat flow calibration. Helium was used as a purge gas. To erase temperature history completely, all the samples were annealed at a temperature higher than the $T_g$ of both blend components. Samples were rapidly cooled down to a temperature below the $T_g$s of both components, at rates higher than 40 °C/min over most of the temperature range. DSC scans were then obtained during heating of the sample at a ramp rate of 10 °C/min, which was followed by a cooling cycle and second heating cycle at the same ramp rate. DSC scans obtained during second heating were compared to first heating scans and were found to be equivalent.

**Rheological Measurements.** Viscoelastic measurements were carried out with an ARES rheometer using parallel plate geometry. Depending upon the modulus of the blend and its proximity to the glass transition temperature, either 25 or 7.94 mm diameter plates were used. The measurements were carried out within the temperature range 0−160 °C, depending upon blend composition. A maximum temperature of 160 °C was chosen in order to avoid any possibility of phase separation in PS/PVME blends and cross-linking of VPh units in the other systems.[62] During measurement the sample was enclosed in a convection oven, and the temperature was controlled by nitrogen gas. For temperatures below room temperature, a special assembly allowing the use of liquid nitrogen was employed. The temperature of the sample during measurements was always kept within ±0.3 °C of the set temperature. Before loading the sample, the gap was zeroed at a certain reference temperature. Sufficient sample was loaded on the plates so as to keep the gap close to 1 mm. During the data analysis, the gap value was adjusted in order to account for thermal expansion of the tools. Strain sweep measurements were carried out to determine the linear viscoelastic region prior to conducting frequency sweeps.

**Fourier Transform Infrared Spectroscopy (FTIR) Measurements.** FTIR measurements were carried out on selected PSVPh80/PVME and PSVPh50/PVME blends, which were of the most interest. Blend samples were dissolved in methyl ethyl ketone (2-butanone, 99.5+%, Sigma-Aldrich) at 2% (w/v) and cast onto potassium bromide (KBr) windows for FTIR analysis. The windows were left in a vacuum oven overnight at 100 °C to remove residual solvent and water. The individual films were then pressed between two KBr windows while still hot, to achieve an even distribution of polymer over the entire area. Films that best obeyed the Beer−Lambert law (maximum absorption ~0.7 in the wavenumber range of interest) were used in this study. Spectra were obtained as a function of temperature using a temperature-controlled, custom-made, horizontal cell (to prevent flow at high temperatures) and a Bio-Rad model FTS-45 Fourier transform infrared (FTIR) spectrometer. Spectra were acquired at a resolution of 1 $cm^{-1}$, with a minimum of 256 interferograms being signal averaged every 10 °C from 40 to 170 °C.

## Results and Discussion

**Rheological Measurements.** The time−temperature superposition principle (tTS) is based on the concept that all polymer relaxations are derived from the same underlying segmental motions and thus exhibit the same temperature

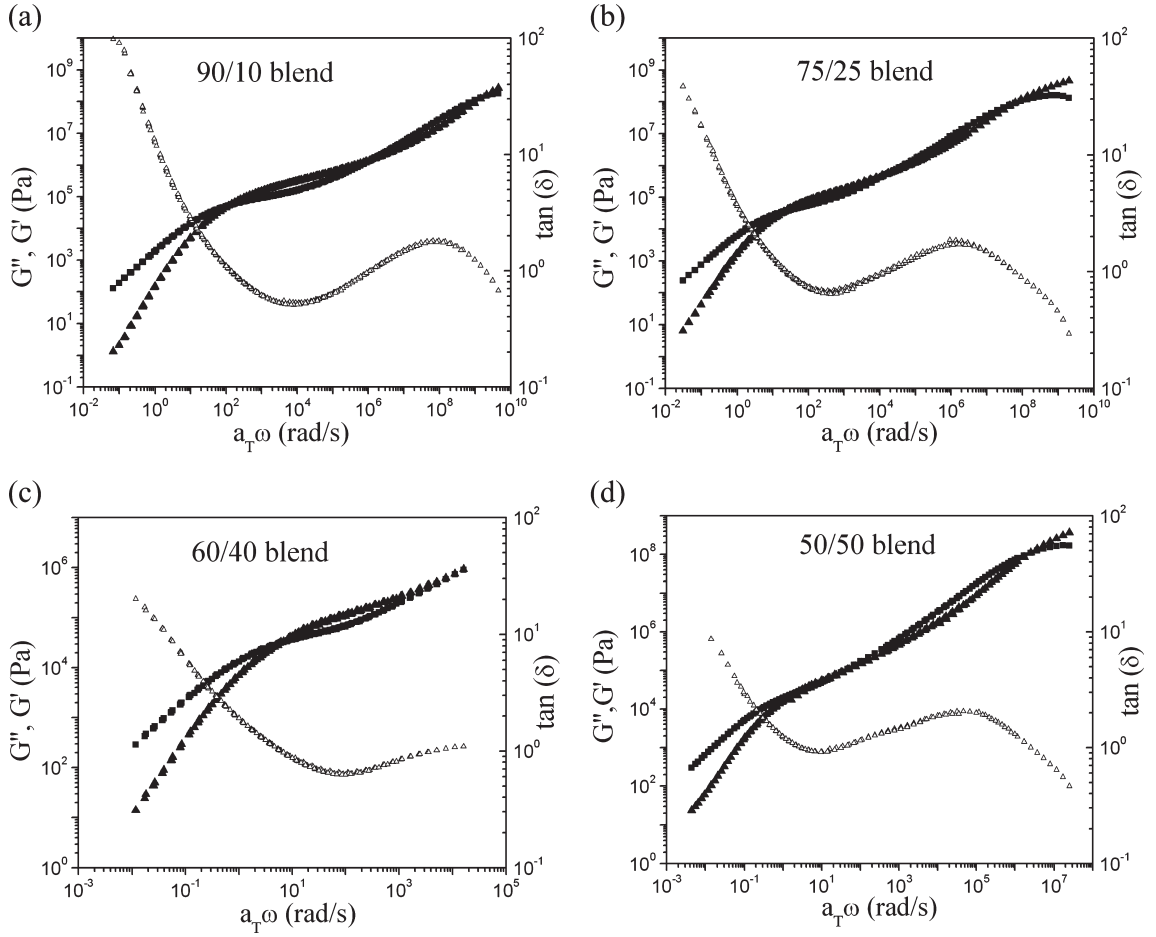


**Figure 3.** Master curves of $G'$ (▲), $G''$ (■), and tan($\delta$) (Δ) for PVME/PSVPh50 blends: (a) 90% PVME; (b) 75% PVME; (c) 60% PVME; (d) 50% PVME. The reference temperature is 100 °C for each curve.

dependence. Under tTS the frequency ($\omega$) dependence of the complex modulus at two different temperatures is given by the simple scaling

$$G^*(\omega, T) = b_T G^*(a_T\omega, T_0) \quad (1)$$

where $T_0$ is the chosen reference temperature and $a_T$ and $b_T$ are the shift factors. The horizontal shift factors $a_T$ were determined by shifting tan($\delta$) data until optimal superposition was observed. Subsequently, an independent vertical shift $b_T$, accounting for density variations, was applied to the modulus data to obtain good master curves. The values of the shift factors are tabulated in the Supporting Information. The storage modulus ($G'$), loss modulus ($G''$), and tan($\delta$) master curves are shown in Figures 1, 2, and 3 for PVME blended with PSPVPh90, PSPVPh80, and PSPVPh50, respectively. All the master curves were created with a reference temperature of 100 °C. The master curves for PS/PVME and PVPh/PVME blends are provided in the Supporting Information, as the viscoelastic properties of both of these systems have been described previously.[37,50]

As can be seen, both $G'$ and $G''$ vary smoothly with frequency and in a qualitatively similar manner in all cases. However, in certain blends, good tan($\delta$) master curves could not be generated. For example, the master curve for the PSVPh90/PVME 50/50 blend in Figure 1d shows a discrepancy in the mid-frequency regime. This failure of tTS principle is very similar to that reported for PS/PVME by Pathak et al.[37] As summarized in Table 2, tTS was obeyed for all the PSVPh50 and PVPh blends, whereas for PS, PSVPh90, and PSVPh80 blends with 40% or 50% PVME, tTS failure was observed.

**Table 2. Applicability of Time−Temperature Superposition[a]**

| | higher $T_g$ component | | | | |
|---|---|---|---|---|---|
| % w/w PVME | PS | PSVPh90 | PSVPh80 | PSVPh50 | PVPh |
| 10 | √ | √ | √ | √ | √ |
| 25 | √ | √ | √ | √ | √ |
| 40 | × | × | × | √ | √ |
| 50 | × | × | × | √ | √ |

[a] √ indicates successful tTS application whereas × indicates failure of tTS.

Differences in the temperature dependences of the rate of relaxation of the two-component polymers in the blend lead to the failure of tTS. Generally, such tTS failure is accentuated when the component $T_g$s are further apart. In this scenario, the PVME/PVPh blends would show the most prominent failure ($\Delta T_g \approx 200$ °C) and PS/PVME ($\Delta T_g \approx 125$ °C) the least, but this is opposite to what is observed. A recent study on PVPh blended with PVME also reported thermorheological simplicity.[50] It is possible to reduce the mobility difference between the two different chains and couple their segmental motions via hydrogen bonding. With sufficient interactions, this could lead to all the chains relaxing with the same underlying segmental times, and tTS would be obeyed. Of course, the determination that tTS "fails" or "succeeds" can have an element of subjectivity, but Figure 4 shows the tan($\delta$) master curves for different systems with same PVME fraction (50 wt %) on an expanded scale. The curves are arbitrarily shifted on the vertical scale

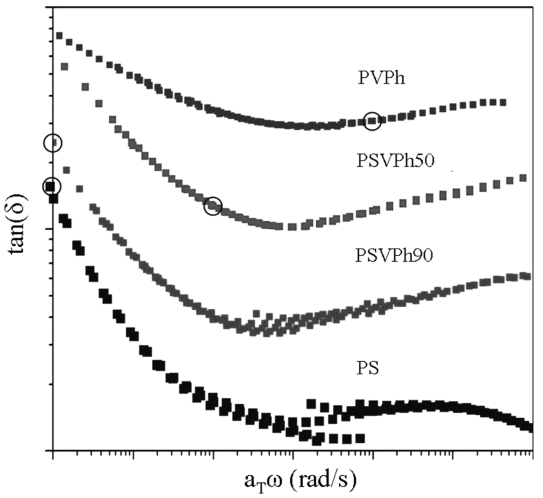


**Figure 4.** Variation of tan(δ) with frequency for different blends with 50% w/w PVME. The curves are shifted vertically for better resolution. The curves are shifted on horizontal axis, but the circle on each curve indicates a point where the reduced frequency is 1.

for better resolution. In the case of PS and PSVPh90, hydrogen-bonding interactions are insufficient to couple the dynamic response and a clear tTS failure is observed, whereas for PSVPh50 and PVPh blends with more hydrogen bonding, tTS is obeyed. The superposition improved with the increase in the hydrogen-bonding interactions, finally resulting in successful application of tTS. Thus, it can be concluded that the dynamic response of the polymers can be coupled with increasing hydrogen-bonding interactions, and that this factor can outweigh the increase in $\Delta T_g$.

**Fourier Transform Infrared Spectroscopy.** Infrared spectroscopy is widely used to study hydrogen bonding in polymers. Significant frequency shifts and changes in the intensities of various bands in the NH and OH stretching region of the spectrum have been observed as a function of temperature. Initially, these changes were interpreted in terms of large changes in absorption coefficients.[63] However, bands due to hydrogen-bonded groups are broad and there appears to be a number of overlapping modes contributing in this region of the spectrum. Recent studies of ethylphenol and PVPh have clarified some of these issues.[64,65] By systematically studying and curve-resolving spectra obtained as a function of composition and temperature, the most prominent bands contributing to the overall profile were identified. In effect, two different types of free and bonded bands were assigned, as discussed in more detail in the Appendix. Based on the calculations outlined in the Appendix and Supporting Information, an estimate for the number of hydrogen-bonding interactions in the blend can be obtained. For example, a plot of the fraction of VPh and PVME segments that are involved in OH−ether hydrogen bonds is shown in Figure 5. These calculations were made for a 50/50 blend at temperatures of 25 and 100 °C. Although the extent of hydrogen bonding decreases with temperature, this decrease is not particularly significant for the hydrogen-bonded PVME units over the temperature range covered in this study. Therefore, data at room temperature provide a reasonable estimate of the fraction of hydrogen-bonded groups.

The values of the radius of gyration, $R_g$, and Kuhn length, $l_k$, for PVME, assuming that it is a Gaussian coil, are approximately 82 and 11 Å, respectively.[69,70] On the basis of the $R_g$ value and number of hydrogen bonded units from the association models, the approximate size of the "control volume", or the volume per hydrogen bond, and the corresponding length

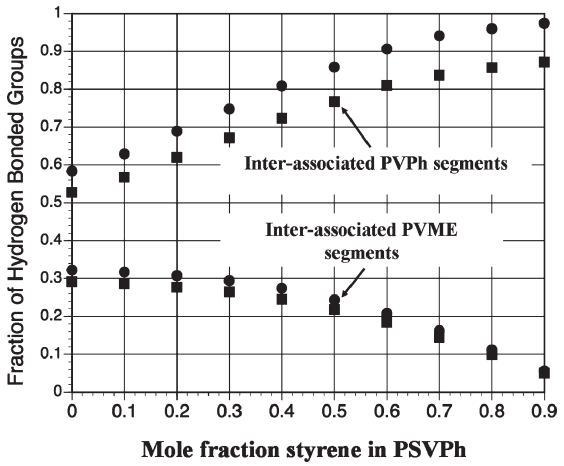


**Figure 5.** Fraction of VPh and PVME segments that are involved in OH−ether hydrogen plotted against the styrene content of the copolymer. Calculations were made for a 50/50 blend at temperatures of 25 °C (circles) and 100 °C (squares).

scale, $l_H$, can be calculated. As noted in Figure 5, for the PSVPh80/PVME 50/50 blend only 1 out of 10 PVME units was hydrogen bonded, and tTS failure was observed. This indicates the presence of heterogeneity on the scale of ∼10 repeat units. The value for $l_H$ is ∼17 Å. On the other hand, from Figure 9, for the PSVPh50/PVME 40/60 blend 1 out of 6 PVME units was hydrogen bonded and tTS was obeyed for this blend. The value for $l_H$ in this case turns out to be ∼14 Å. This length scale is comparable to the Kuhn length. This result is at least consistent with an underlying assumption of the self-concentration model for miscible blends,[13] in which the relevant length scale is given by the Kuhn length.

In a previous study on PVPh/PVME blends, segmental dynamics were probed using broadband dielectric spectroscopy.[71] At low concentrations of PVPh, a fast relaxation phenomenon was observed which was assigned to the non-hydrogen-bonded PVME units. However, it was reported that dynamic homogeneity was obtained when 30% PVPh was present in the blend. According to the association models for that particular system, at this blend composition ∼22% of the PVME units were hydrogen bonded, which is more than one hydrogen bond per Kuhn length cubed. Therefore, this observation is also consistent with our conclusions regarding the number of hydrogen bonds needed to impart thermorheological simplicity in the PVPh/PVME blend system.

## Conclusions

Viscoelastic measurements have been presented for blends of PVME with PS, PVPh, and PSVPH statistical copolymers. By controlling the percent styrene in the copolymer, the extent of hydrogen-bonding interactions was effectively modulated. The time−temperature superposition (tTS) principle is known to fail in PS/PVME blends, with no hydrogen bonding, and to succeed in PVME/PVPh blends, with extensive hydrogen bonding. This is the case despite the fact that the difference between component glass transition temperatures is significantly greater in the latter system. For blends containing 50% PVME, tTS is found to fail with PS, and with statistical copolymers containing 90% and 80% styrene, but tTS is successful for blends with PVPh and with a statistical copolymer containing 50% styrene. By using a well-established model for hydrogen bonding in polymer blends, it was possible to estimate the concentration of hydrogen bonds in these various systems and thereby to obtain a "critical concentration" of hydrogen bonds necessary to restore the applicability of tTS.

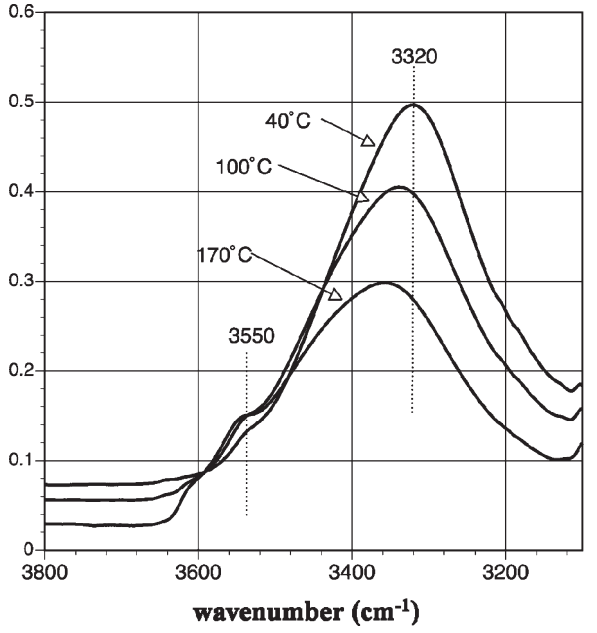


**Figure 6.** Infrared spectra of PSVPh50/PVME blends (50% w/w) obtained at 40, 100, and 170 °C.

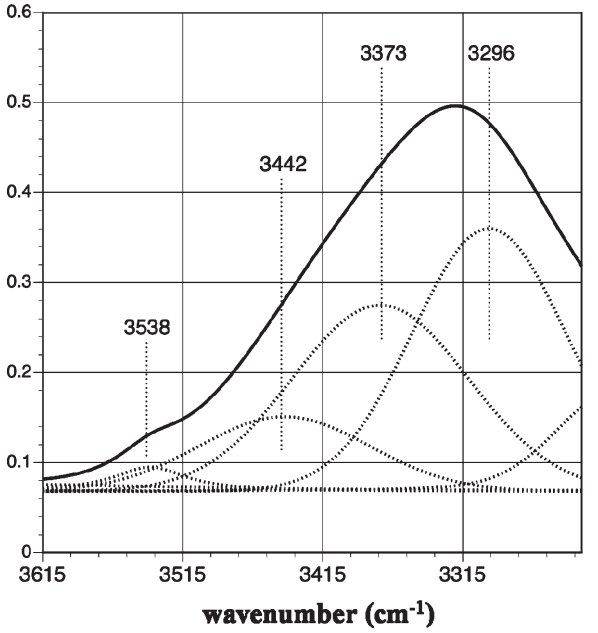


**Figure 7.** Infrared spectrum of the PSVPh50/PVME (50%) blend obtained at 40 °C curve-resolved into its component bands.

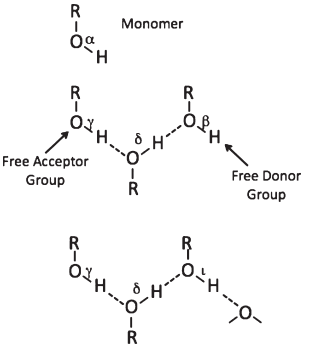


**Figure 8.** Schematic representation of the types of hydrogen-bonded groups found in PSPVPh/PVME blends.

This concentration corresponds closely to one hydrogen bond per Kuhn length cubed.

**Acknowledgment.** This work was supported by the National Science Foundation through Award DMR-0804197. The assistance of Dr. David Giles with the rheological and calorimetric measurements is appreciated.

**Supporting Information Available:** Text giving additional details of the synthesis and characterization of the polymers, the viscosity of certain blends, and the model for computing numbers of hydrogen bonds, figures showing SEC chromatograms, NMR spectra, blend viscosities, and tan $\delta$ for various blends, tables including glass transition values and widths, time−temperature superposition shift factors, and hydrogen-bonding equilibrium constants. This material is available free of charge via the Internet at http://pubs.acs.org.

## Appendix. Fourier Transform Infrared Spectroscopy Analysis

The problems associated with curve-fitting complex band profiles, and the methods used to mitigate them, were discussed in detail in previous studies dealing with the OH stretching region of ethyl phenol and PVPh.[64,65] The same methodology was used here, and a chosen region of the spectrum was fit using a function that is a sum of Lorentzian and Gaussian band shapes.

As noted in Table 2, tTS failed for PS/PVME, PSVPh90/PVME, and PSVPh80/PVME 50%/50% w/w blends, whereas the master curve improved with increase in hydrogen-bonding interactions, such that tTS was obeyed for PSVPh50 and PVPh blends with 50 wt % PVME. For blends with even lower amounts (10% or 25%) of PS, PSVPh90 or PSVPh80, tTS failure was not observed prominently, even though it might be expected. This is due to fact that the high $T_g$ component may not be present in sufficient amount to generate a significant contribution to the observed moduli in this frequency range. Thus, the blends of PSVPh80 and PSVPh50 with PVME were determined to be of paramount interest.

Infrared spectra of PSVPh50/PVME and PSVPh80/PVME blends (50% of each component) were obtained as a function of temperature in the range 40−170 °C. As examples, spectra of the PSVPh50/PVME blend recorded at 40, 100, and 170 °C are shown in Figure 6. It can be seen that as the temperature is increased, the peak position of maximum absorption, near 3320 $cm^{-1}$ at room temperature, shifts to higher wavenumbers. The strongest band in the spectrum of PVPh at room temperature is near 3350 $cm^{-1}$, and the shift to lower frequency in the spectrum of the blends is a result of the formation of OH−ether hydrogen bonds, which are stronger than their OH−OH counterparts. The intensity of maximum absorption also decreases significantly with increasing temperature. In contrast, the bands contributing to shoulders near 3550 and 3660 $cm^{-1}$ become more intense with increasing temperature. Bands in this region of the spectrum are usually associated with "free" or non-hydrogen-bonded OH groups.

The results of curve resolving the spectrum obtained at 40 °C are shown in Figure 7. The most intense bands were determined to be Gaussian, as in a previous study of PVPh.[65] These bands can be readily assigned to various types of hydrogen-bonded or free groups based on a previous study of PVPh, which in turn used an approach to band assignments of OH groups used by Hall and Wood[66] and Ohta and Tominaga.[67] In these reports, four functionally different groups, which were labeled as $\alpha$, $\beta$, $\gamma$, and $\delta$, illustrated schematically in Figure 8, were identified. To these, we have added a fifth group, labeled $\iota$, to describe OH−ether hydrogen bonds. The $\alpha$ group corresponds to the monomer, where neither the oxygen atom nor the proton of an OH group is

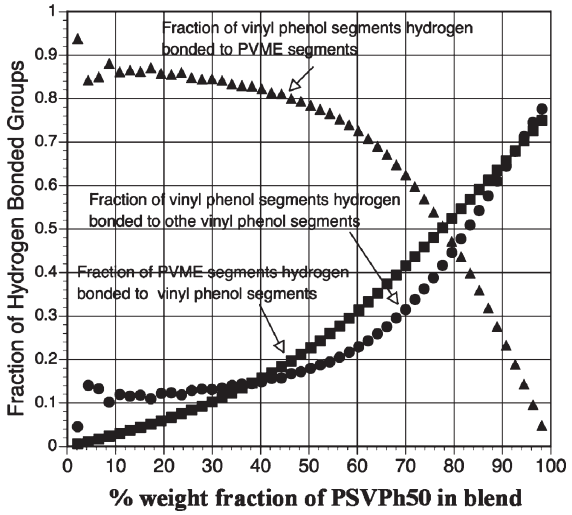


**Figure 9.** Fraction of hydrogen-bonded groups of various types plotted as a function of blend composition at 40 °C for a 50 wt % blend of PSVPh50/PVME.

involved in hydrogen bonding; the $\beta$ group corresponds to an end group where the proton is not acting as a donor, but the oxygen atom acts as an acceptor; the $\gamma$ group to an end group where the proton is acting as a donor, while the oxygen atom is not acting as an acceptor; the $\delta$ group is where both the oxygen atom and proton act as acceptor and donor, respectively.

In the spectra of the blends we could not distinguish between $\alpha$ and $\beta$ free OH groups. Furthermore, because OH groups can form weak hydrogen bonds to aromatic $\pi$-orbitals, we observe a free OH band near 3600 $cm^{-1}$ and an OH-$\pi$ group near 3538 $cm^{-1}$.[65] The former is almost invisible at room temperature but is easily seen at higher temperatures (see Figure 6). Both increase in intensity as the temperature of the sample is raised. The bands near 3442 and 3373 $cm^{-1}$ (at 40 °C) can be assigned to $\gamma$ groups (where the proton is acting as a donor, while the oxygen atom is not acting as an acceptor) and $\delta$ groups (where both the oxygen atom and proton act as acceptor and donor, respectively), respectively. The band curve resolved near 3296 $cm^{-1}$ (again at 40 °C) is assigned to $\iota$ groups, interassociated OH−ether hydrogen-bonded OH stretching modes.

Also, as observed in a previous study, most of the changes in the OH stretching region of the spectrum with temperature are a result of a change in the distribution of hydrogen-bonded and free species, rather than changes in absorption coefficients.[65] In order to relate the intensities of these various OH stretching modes to the concentration of corresponding OH hydrogen-bonded species, one would need to know the absorption coefficients for each mode. These are presently unknown. However, the experimental results are consistent with the number of OH−OH and OH−ether hydrogen bonds calculated using the equilibrium constants determined in previous work[52] and modified to account for self-concentration.[68] More details about the model and the parameters used can be found in the Supporting Information.

The calculated fraction of hydrogen-bonded groups of various types for PSVPh50/PVME blends at 40 °C is shown as a function of blend composition in Figure 9. It can be seen that the fraction of OH groups hydrogen bonded to ether oxygen groups is significantly larger than the fraction of OH groups engaged in OH/OH hydrogen bonds, in accord with spectroscopic observations. Interestingly, a far larger fraction of vinylphenol units are hydrogen bonded to ether oxygen groups than PVME groups are hydrogen bonded to phenolic OH groups. This is a consequence of the large difference in molar volume of the units in the copolymer and PVME segments. At a composition of 50 wt % there are almost twice as many PVME segments than VPh or styrene segments.

## References and Notes

(1) Rouse, P. E. *J. Chem. Phys.* **1953**, *21*, 1272.
(2) Doi, M.; Edwards, S. F. *The Theory of Polymer Dynamics*; Oxford University Press: Oxford, 1986.
(3) Colby, R. H. *Polymer* **1989**, *30*, 1275.
(4) He, Y.; Lutz, T. R.; Ediger, M. D. *J. Chem. Phys.* **2003**, *119*, 9956.
(5) Roovers, J.; Toporowski, P. M. *Macromolecules* **1992**, *25*, 1096.
(6) Roovers, J.; Toporowski, P. M. *Macromolecules* **1992**, *25*, 3454.
(7) Haley, J. C.; Lodge, T. P.; He, Y.; Ediger, M. D. *Macromolecules* **2003**, *36*, 6142.
(8) Zawada, J. A.; Fuller, G. G.; Colby, R. H.; Fetters, L. J.; Roovers, J. *Macromolecules* **1994**, *27*, 6851.
(9) Zawada, J. A.; Fuller, G. G.; Colby, R. H.; Fetters, L. J.; Roovers, J. *Macromolecules* **1994**, *27*, 6861.
(10) Chung, G. C.; Kornfield, J. A.; Smith, S. D. *Macromolecules* **1994**, *27*, 5729.
(11) Chung, G. C.; Kornfield, J. A.; Smith, S. D. *Macromolecules* **1994**, *27*, 964.
(12) Kim, E.; Kramer, E. J.; Wu, W. C.; Garret, P. D. *Polymer* **1994**, *35*, 5706.
(13) Lodge, T. P.; McLeish, T. C. B. *Macromolecules* **2000**, *33*, 5278.
(14) Liu, C.; Wang, J.; He, J. *Polymer* **2002**, *43*, 3811.
(15) Wu, S. *Polymer* **1987**, *28*, 1144.
(16) Yang, H. H.; Han, C. D.; Kim, J. K. *Polymer* **1994**, *35*, 1503.
(17) Aoki, Y.; Tanaka, T. *Macromolecules* **1999**, *32*, 8560.
(18) Kataoka, T.; Ueda, S. *J. Polym. Sci., Polym. Chem.* **1967**, *5*, 3071.
(19) Prest, W. M., Jr. *J. Polym. Sci., Polym. Phys.* **1970**, *8*, 1897.
(20) Hoffmann, M. *Makromol. Chem.* **1972**, *153*, 99.
(21) Friedman, E. M.; Porter, R. S. *Trans. Soc. Rheol.* **1975**, *19*, 493.
(22) Wu, S. *J. Polym. Sci., Polym. Phys.* **1987**, *25*, 557.
(23) Aoki, Y. *Macromolecules* **1990**, *23*, 2309.
(24) Wisniewsky, C.; Marin, G.; Monge, P. *Eur. Polym. J.* **1984**, *20*, 691.
(25) Han, C. D.; Yang, H. H. *J. Appl. Polym. Sci.* **1987**, *33*, 1199.
(26) Wu, S. *J. Polym. Sci., Polym. Phys.* **1987**, *25*, 2511.
(27) Chuang, H. K.; Han, C. D. *J. Appl. Polym. Sci.* **1984**, *29*, 2205.
(28) Pathak, J. A.; Colby, R. H.; Kamath, S. Y.; Kumar, S. K.; Stadler, R. *Macromolecules* **1998**, *31*, 8988.
(29) Alegria, A.; Colmenero, J.; Ngai, K. L.; Roland, C. M. *Macromolecules* **1994**, *27*, 4486.
(30) Ngai, K. L.; Plazek, D. J. *Macromolecules* **1990**, *23*, 4282.
(31) Ajji, A.; Choplin, L.; Prud'homme, R. E. *J. Polym. Sci., Polym. Phys.* **1988**, *26*, 2279.
(32) Ajji, A.; Choplin, L.; Prud'homme, R. E. *J. Polym. Sci., Polym. Phys.* **1991**, *29*, 1573.
(33) Roland, C. M.; Ngai, K. L. *Macromolecules* **1992**, *25*, 363.
(34) Kim, J. K.; Lee, H. H.; Son, H. W.; Han, C. D. *Macromolecules* **1998**, *31*, 8566.
(35) Cavallie, J. Y.; Perez, J.; Jourdan, C.; Johari, G. P. *J. Polym. Sci., Polym. Phys.* **1987**, *25*, 1847.
(36) Takahashi, Y.; Suzuki, H.; Nakagawa, Y.; Noda, I. *Macromolecules* **1994**, *27*, 6476.
(37) Pathak, J. A.; Colby, R. H.; Floudas, G.; Jerome, R. *Macromolecules* **1999**, *32*, 2553.
(38) Trask, C. A.; Roland, C. M. *Macromolecules* **1989**, *22*, 256.
(39) Arendt, B. H.; Krishnamoorti, R.; Kornfield, J. A.; Smith, S. D. *Macromolecules* **1997**, *30*, 1127.
(40) Roland, C. M.; Ngai, K. L. *Macromolecules* **1991**, *24*, 2261.
(41) Sy, J. W.; Mijovic, J. *Macromolecules* **2000**, *33*, 933.
(42) Carini, G.; D'Angelo, G.; Tripodo, G.; Bartolotta, A.; Di Marco, G.; Lanza, M.; Privalko, V. P.; Gorodilov, B, Y.; Rekhteta, N. A.; Privalko, E. G. *J. Chem. Phys.* **2002**, *116*, 7316.
(43) Qiu, F.; Chen, S.; Tan, L.; Ping, Z. *Polym. Adv. Technol.* **2004**, *15*, 453.
(44) Prinos, A.; Dompros, A.; Panayiotou, C. *Polymer* **1998**, *39*, 3011.
(45) Cai, H.; Ait-Kadi, A.; Brisson, J. *J. Appl. Polym. Sci.* **2004**, *93*, 1623.
(46) Cai, H.; Ait-Kadi, A.; Brisson, J. *Polymer* **2003**, *44*, 1481.
(47) Brisson, J. *Polym. Eng. Sci.* **2004**, *44*, 241.
(48) Gestoso, P.; Brisson, J. *Polymer* **2001**, *42*, 8415.
(49) Zhang, S. H.; Jin, X.; Painter, P. C.; Runt, J. *Polymer* **2004**, *45*, 3933.
(50) Yang, Z.; Han, C. D. *Macromolecules* **2008**, *41*, 2104.
(51) Li, D.; Brisson, J. *Macromolecules* **1997**, *30*, 8425.

(52) Coleman, M. M.; Graf, J. F.; Painter, P. C. *Specific Interactions and the Miscibility of Polymer Blends*; Technomic Publishing Inc.: Lancaster, PA, 1991.
(53) Cavaille, J. Y.; Corrinne, J.; Perez, J.; Monnerie, L.; Johari, G. P. *J. Polym. Sci., Polym. Phys.* **1987**, *25*, 1235.
(54) Stadler, R.; Freitas, L. D.; Krieger, V.; Klotz, S. *Polymer* **1988**, *29*, 1643.
(55) Zetsche, A.; Fischer, E. W. *Acta Polym.* **1994**, *45*, 168.
(56) Zetsche, A.; Kremer, F.; Jung, W.; Schulze, H. *Polymer* **1990**, *31*, 1883.
(57) Roland, C. M.; Ngai, K. L. *Prog. Colloid Polym. Sci.* **1993**, *91*, 75.
(58) Zhang, S. H.; Painter, P. C.; Runt, J. P. *Macromolecules* **2004**, *37*, 2636.
(59) Davidock, D. Ph.D. Thesis, University of Minnesota, **2004**.
(60) Ohno, K.; Ejaz, M.; Fukuda, T.; Miyamato, T.; Shimizu, Y. *Macromol. Chem. Phys.* **1998**, *199*, 291.
(61) Yoshida, E.; Takiguchi, Y. *Polymer* **1999**, *31*, 429.
(62) Still, R. H.; Whitehead, A. *J. Appl. Polym. Sci.* **1977**, *21*, 1215.
(63) Coleman, M. M.; Skrovanek, D. J.; Howe, S. E.; Painter, P. C. *Macromolecules* **1985**, *18*, 299.
(64) Choperena, A.; Painter, P. C. *Vib. Spectrosc.* **2009**, *51*, 110.
(65) Choperena, A.; Painter, P. *Macromolecules* **2009**, *42*, 6159.
(66) Hall, A.; Wood, J. L. *Spectrochim. Acta* **1967**, *23A*, 2657.
(67) Ohta, K.; Tominaga, K. *Chem. Phys.* **2007**, *341*, 310.
(68) Painter, P. C.; Coleman, M. M. *Polymer Blends: Formulation and Performance*; Paul, D. R., Bucknall, C. B., Eds.; John Wiley & Sons: New York, 1999.
(69) Zhang, S.; Painter, P. C.; Runt, J. P. *Macromolecules* **2002**, *35*, 9403.
(70) Fetters, L. J.; Lohse, D. J.; Graessley, W. W. *J. Polym. Sci., Polym. Phys.* **1999**, *37*, 1023.
(71) Zhang, S. H.; Jin, X.; Painter, P. C.; Runt, J. P. *Macromolecules* **2003**, *36*, 5710.
(72) Mpoukouvalas, K.; Floudas, G.; Zhang, S. H.; Runt, J. *Macromolecules* **2005**, *38*, 552.